Photosensitizers for H_2 evolution based on charged or neutral Zn and Sn porphyrins

Emmanouil Gianoudis,[a,b] Elisabetta Benazzi,[c] Joshua Karlsson,[c] Graeme Copley,[c] Stylianos Panagiotakis,[a] Georgios Landrou,[a] Panagiotis Angaridis,[d] Vasilis Nikolaou,[a] Chrysanthi Matthaiaki, [a] Georgios Charalambidis,*[a] Elizabeth A. Gibson,*[c] Athanassios G. Coutsolelos*[a]

[a]Laboratory of Bioinorganic Chemistry, Department of Chemistry, University of Crete, Voutes Campus, 70013 Heraklion, Crete, Greece, E-mail: acoutsol@uoc.gr

[b]Laboratoire de Chimie et Biologie des Métaux, UMR 5249 Université Grenoble Alpes, CNRS, CEA, 17 rue des Martyrs, F-38054 Grenoble Cedex 9, France.

[c]Chemistry – School of Natural and Environmental Sciences, Newcastle University, NE1 7RU United Kingdom, E-mail: elizabeth.gibson@newcastle.ac.uk.

[d]Department of Chemistry, Aristotle University of Thessaloniki, Thessaloniki 54124, Greece.

Corresponding Author

E-mail: acoutsol@uoc.gr (A.G.C.)

E-mail: gcharal@uoc.gr (G.C.)

E-mail: elizabeth.gibson@newcastle.ac.uk (E.A.G.)

Keywords: zinc, tin, porphyrin, hydrogen production, photosensitizer, catalyst, cobalt complex, transient absorption measurements, photophysical investigation, electrochemistry

ABSTRACT

We report a comparison between a series of zinc and tin porphyrins as photosensitizers for photochemical hydrogen evolution using cobaloxime complexes as molecular catalysts. Among all the chromophores tested, only the positively charged zinc porphyrin, **[ZnTMePyP^{+}]Cl$_4$**, and the neutral tin porphyrin derivatives, **Sn(OH)$_2$TPyP**, **Sn(Cl$_2$)TPP-[COOMe]$_4$** and **Sn(Cl$_2$)TPP-[PO(OEt)$_2$]$_4$**, were photocatalytically active. Hydrogen evolution was strongly affected by the pH value as well as the different concentrations of both the sensitizer and the catalyst. A comprehensive photophysical and electrochemical investigation was conducted in order to examine the mechanism of photocatalysis. The results derived from this study establish fundamental criteria with respect to the design and synthesis of porphyrin derivatives for their application as photosensitizers in photo-induced hydrogen evolution.

INTRODUCTION

Coupling energy storage with power generation from renewable and abundant energy sources is becoming increasingly urgent and artificial photosynthesis, generating fuel with sunlight, is one potential solution.[1,2] The use of hydrogen as an energy vector is a technically feasible approach to help satisfy the rapidly growing global energy demand.[3] A direct method of generating hydrogen and oxygen via water splitting using solar irradiation is under development. However, important challenges still need to be addressed before a low-cost, highly efficient and environmentally benign technology is established.[4,5]

The photo-induced water splitting and proton reduction processes are mainly driven by systems consisting of three main components. More specifically, a sacrificial electron donor (**SED**), a light harvesting unit (photosensitizer, **PS**) and a hydrogen evolution catalyst (**HEC**).[6] The appropriate choice of the PS is a crucial parameter in light-driven proton reduction. Complexes consisting of Ru, Ir, Re or Pt metals are the most widely employed chromophores in such schemes, but the use of noble metals may limit the application of artificial photosynthesis on an industrial scale.[5,7-15] However, porphyrins or other macrocyclic derivatives based on earth abundant elements are potentially more sustainable sensitizers in photocatalytic systems.[16-25] The metallation of the porphyrin with, for example,Mg(II), Zn(II) or Sn(IV) ensures good stability and, together with the modification of the periphery with appropriate functional groups, can tune the excited-state properties.[26] Accordingly, Zn(II) and Sn (IV) porphyrins have been developed as artificial light-harvesting units for proton reduction, due to their versatility, they absorb solar energy efficiently and possess suitable redox potentials for water splitting.[27,28] In addition, Sn (IV) porphyrins possess extra stability as the large, highly-charged, Sn^{4+} cation fits perfectly into the porphyrin macrocycle.[29] Furthermore, the long-lived triplet excited state of these metalloporphyrins is an

important requirement for efficient hydrogen photogeneration systems.[30] A number of molecular catalysts have shown remarkable efficiency towards photo-induced hydrogen production. The most noteworthy examples are noble metal-free molecular Co or Ni-based systems, which are able to reduce protons efficiently.[19,31-34] Cobalt complexes with diglyoxime ligands (cobaloximes) are one well-documented class of catalysts for hydrogen evolution,[16,35] which are quite stable, can be readily synthesized using straightforward preparation methods and contain an inexpensive transition-metal.[16,35]

Our group has thoroughly studied various photocatalytic hydrogen production systems, including the application of water-soluble **Zn(II)** and **Sn(IV)** porphyrins as photosensitizers combined with cobalt catalysts.[16-18] In this new study we have synthesized Zn and Sn porphyrin sensitizers, in order to investigate the influence of the charge of the *para*-substituents of meso-phenyl groups of the porphyrin and to explore the impact that these modifications will have on the performance of the system towards photo-induced hydrogen evolution. The porphyrins studied are presented in Figure 1, neutral (**ZnTPyP**, **ZnTPP-[COOMe]$_4$**, **ZnTPP-[PO(OEt)$_2$]$_4$**, **Sn(OH)$_2$TPyP**, **Sn(Cl$_2$)TPP-[COOMe]$_4$**, **Sn(Cl$_2$)TPP-[PO(OEt)$_2$]$_4$**), positively charged (**[ZnTMePyP$^+$]Cl$_4$**, **[Sn(OH)$_2$TMePyP$^+$]Cl$_4$**) and negatively charged (**ZnTPP-[COOH]$_4$**, **Sn(Cl$_2$)TPP-[COOH]$_4$**). The positively charged peripheral substituent chosen was the *N*-methyl pyridyl group, whereas the carboxylate ion was selected as the negatively charged group. Finally, the neutral substituents chosen for this study were pyridyl, methyl ester and phosphate ester. We were able to optimize the photocatalytic activity by tuning both the pH of the buffer solution as well as the concentration of the **PS** and the **HER** catalyst. Photophysical and electrochemical measurements were applied to determine whether there is a pattern in which the charged or neutral porphyrins are effective as photosensitizers in photocatalytic H_2 production.

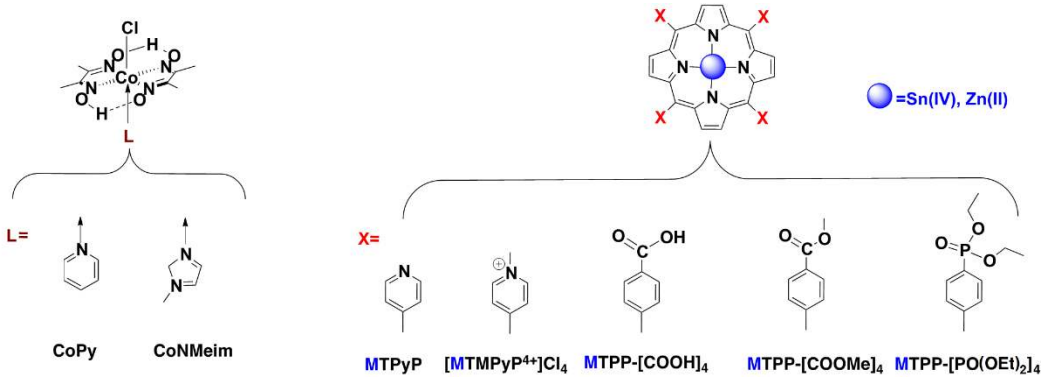

Figure 1. Molecular structure of cobaloxime catalysts, **Zn** and **Sn** porphyrin photosensitizers used for hydrogen evolution.

RESULTS AND DISCUSSION

Synthesis

Ten zinc and tin porphyrin derivatives and two cobaloximes (Figure 1) were synthesized and their performance towards photocatalytic hydrogen evolution was evaluated. The preparation of all *meso*-substituted porphyrins was based on typical Adler-Longo conditions, namely the condensation of pyrrole with the corresponding aldehydes in propionic acid under reflux conditions. The porphyrin derivatives **H_2TPyP**, **H_2TPP-[COOMe]$_4$** and **H_2TPP-[PO(OEt)$_2$]$_4$** were metallated using $Zn(CH_3COO)_2 \cdot 2H_2O$ yielding the corresponding **ZnTPyP**, **ZnTPP-[COOMe]$_4$** and **ZnTPP-[PO(OEt)$_2$]$_4$** derivatives, respectively.[36-39] For the metallation of **H_2TPyP**, **H_2TPP-[COOH]$_4$,** **H_2TPP-[COOMe]$_4$** and **H_2TPP-[PO(OEt)$_2$]$_4$** with tin, each porphyrin derivative was refluxed in pyridine using $SnCl_2$ to afford the metallated porphyrins **Sn(Cl_2)TPyP**, **Sn(Cl_2)TPP-[COOH]$_4$,** **Sn(Cl_2)TPP-[COOMe]$_4$**[18,40-43] and **Sn(Cl_2)TPP-[PO(OEt)$_2$]$_4$** (Figure S1). The dichloro tin(IV) porphyrin **Sn(Cl_2)TPyP** was then treated with K_2CO_3 to afford the dihydroxo tin(IV) porphyrin **Sn(OH)$_2$TPyP**, in order to increase the solubility of this derivative in aqueous solution. The positively charged porphyrins [**ZnTMePyP$^+$**]**Cl$_4$** and [**Sn(OH)$_2$TMePyP$^+$**]**Cl$_4$** were synthesized by methylation of the *N* atoms on pyridyl groups of **ZnTPyP** and **Sn(OH)$_2$TPyP**, respectively. In addition, basic hydrolysis of the ester groups converted the neutral porphyrin **ZnTPP-[COOMe]$_4$** to the negatively charged porphyrin **ZnTPP-[COOH]$_4$**.

All compounds were fully characterized by NMR spectroscopy and MALDI-TOF mass spectrometry while the ^{1}H NMR of **H_2TPP-[PO(OEt)$_2$]$_4$** is depicted in Figure S3. In addition, the metallation of **H_2TPP-[PO(OEt)$_2$]$_4$** with tin was confirmed via UV-visible absorption spectroscopy as shown in Figure S4.

X-ray crystallography

Single-crystals of porphyrin **Sn(Cl_2)TPP-[COOMe]$_4$**, suitable for X-ray crystallographic analysis, were obtained by slow evaporation of a CH_2Cl_2/n-Hexane solution, over a period of two weeks. Details of the crystal data and structure refinement parameters are shown in Table S1. A drawing of the molecular structure of the compound is shown in Figure 2, while selected bond distances and angles are listed in Table S2. Porphyrin **Sn(Cl_2)TPP-[COOMe]$_4$** was crystallized in the triclinic space group P-1 in the form **Sn(Cl_2)TPP-[COOMe]$_4$**$\cdot 2CH_2Cl_2$. It consists of a central Sn atom coordinated by four pyrrole N atoms that form a planar ring, and two Cl atoms at perpendicular positions with respect to the plane of the macrocyclic ring. The metal atom lies on a crystallographic inversion center and it has almost ideal octahedral coordination geometry. This results in essentially identical Sn–N(pyrrole) bond lengths (2.080(4) and 2.081(4) Å) and Sn–Cl

bond lengths (2.4286(15) Å). Bond angles around the metal center are very close to the ideal values of an octahedron (e.g. N1–Sn1–N2 = 90.00(14)°, N1–Sn1–Cl1 = 90.25(12)°, and Cl1–Sn1–Cl1a = 180.0°). All other bond lengths and angles fall within the usual ranges. The 4-methyl-benzoate groups attached to the four meso positions at the periphery of the porphyrin macrocycle were found to be in a tilted orientation with respect to the porphyrin framework, making dihedral angles of ~69° and ~115°.

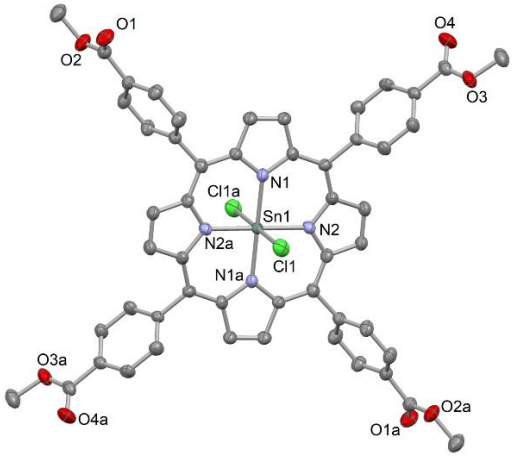

Figure 2. ORTEP view of molecular structure of **Sn(Cl$_2$)TPP-[COOMe]$_4$** with thermal ellipsoids drawn at the 35% probability level. Hydrogen atoms are omitted for clarity.

Absorption and emission properties

The photophysical properties of all dyes were investigated initially through steady state absorption and emission studies. The UV-Visible absorption measurements were performed in 1:1 CH_3CN:H_2O solutions and their normalized spectra are depicted in Figure 3. The spectra of both zinc and tin porphyrins showed the characteristic absorption features of metallated porphyrin macrocycles with two Q bands lying between 550 and 650 nm and one broad peak around 415-425 nm, which corresponds to the Soret band.

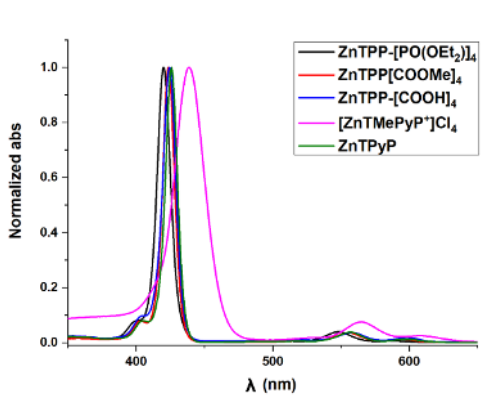

A)

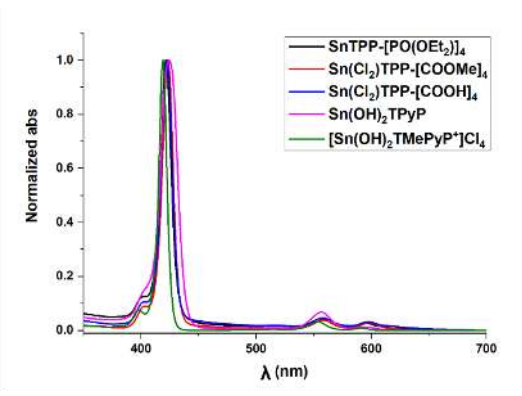

B)

Figure 3. The UV-Visible absorption spectra of the (A) Zn and (B) Sn porphyrins dissolved in MeCN:H_2O 1:1, 5% TEOA, pH=7 solution. In the case of TPyP and [COOMe] derivatives a few drops of THF were used for absolute solubility.

Likewise, the emission properties of all Sn and Zn porphyrins were characteristic of metalloporphyrins.[26] Two emission bands were observed at approximately 600 and 660 nm in each case (Figure 4) following excitation at the corresponding Soret band of each porphyrin. The small Stokes shift between the peak of the absorption band at lower energy and the peak of the emission band at higher energy, confirms the rigidity of these systems and minimal molecular structure distortions during the absorption and emission processes. The absorption and emission data regarding all porphyrin derivatives are summarized in Table 1. [18,36-43]

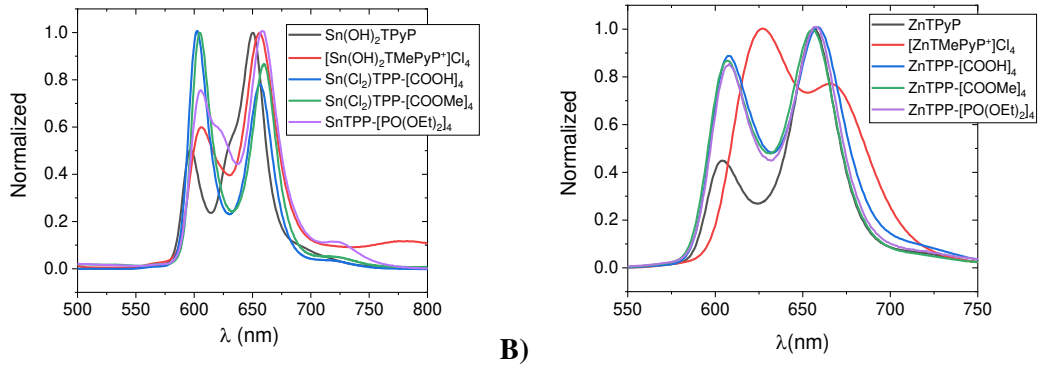

A) **B)**

Figure 4. (A) Emission spectra of tin porphyrins in 1:1 $CH_3CN:H_2O$; Black: **$Sn(OH)_2TPyP$** (λ_{ex} = 417 nm); Red: **$[Sn(OH)_2TMePyP^+]Cl_4$** (λ_{ex} = 422 nm); Blue: **$Sn(Cl_2)TPP\text{-}[COOH]_4$** ($\lambda_{ex}$ = 421 nm); Green: **$Sn(Cl_2)TPP\text{-}[COOMe]_4$** ($\lambda_{ex}$ = 423 nm); Violet: **$Sn(Cl_2)TPP\text{-}[PO(OEt)_2]_4$** ($\lambda_{ex}$ = 424 nm). (B) Emission spectra of zinc porphyrins in 1:1 $CH_3CN:H_2O$; Black: **SnTPyP** (λ_{ex} = 418 nm); Red: **$[ZnTMePyP^+]Cl_4$** (λ_{ex} = 438 nm); Blue: **$ZnTPP\text{-}[COOH]_4$** (λ_{ex} = 421 nm); Green: **$ZnTPP\text{-}[COOMe]_4$** (λ_{ex} = 423 nm); Violet: **$ZnTPP\text{-}[PO(OEt)_2]_4$** ($\lambda_{ex}$ = 424 nm).

Finally, from the spectroscopic data recorded in 1:1 $CH_3CN:H_2O$ solution the energy for the zero-zero electronic transition, E_{00}, between the ground and singlet excited state was estimated, which corresponds to the energy separation between the HOMO and LUMO (see Table 2).

Table 1. Absorption and emission data

Compound	λ_{Soret}/nm[a]	λ_Q/nm[a]	λ_{em}/nm[a]
$Sn(OH)_2TPyP$	417	554/594	597/650
$[Sn(OH)_2TMePyP^+]Cl_4$	422	555/595	606/657
$Sn(Cl_2)TPP\text{-}[COOH]_4$	421	556/596	602/657
$Sn(Cl_2)TPP\text{-}[COOMe]_4$	425	560/600	604/660
$Sn(Cl_2)TPP\text{-}[PO(OEt)_2]_4$	424	560/600	605/659

ZnTPyP	418	555/595	603/656
[ZnTMePyP$^+$]Cl$_4$	438	565/608	627/667
ZnTPP-[COOH]$_4$	421	558/597	608/659
ZnTPP-[COOMe]$_4$	423	557/597	607/657
ZnTPP-[PO(OEt)$_2$]$_4$	424	558/598	608/657

[/a]concentration: 5 x 10^{-5} M in 1:1 CH_3CN/H_2O

Hydrogen evolution

In our previously published works, the combination of water soluble porphyrin photosensitizers, **Sn(OH)$_2$TPyP** and **[ZnTMePyP$^+$]Cl$_4$**, with a cobaloxime catalyst and triethanolamine (**TEOA**) as a sacrificial electron donor, exhibited high photocatalytic activity towards hydrogen evolution.[16-18] These promising results inspired us to examine neutral (**ZnTPyP**, **ZnTPP-[COOMe]$_4$**, **ZnTPP-[PO(OEt)$_2$]$_4$**, **Sn(OH)$_2$TPyP**, **Sn(Cl$_2$)TPP-[COOMe]$_4$** and **Sn(Cl$_2$)TPP-[PO(OEt)$_2$]$_4$**), positively charged (**[ZnTMePyP$^+$]Cl$_4$** and **[Sn(OH)$_2$TMePyP$^+$]Cl$_4$**) and negatively charged (**ZnTPP-[COOH]$_4$** and **Sn(Cl$_2$)TPP-[COOH]$_4$**) zinc and tin *meso*-substituted porphyrins as photosensitizers. It is worth mentioning that **Sn(Cl$_2$)TPP-[COOH]$_4$** is neutral after the synthesis conditions, but in the mixture that the photocatalytic experiments were conducted is negatively charged, since the peripheral carboxylate groups have a pKa of ca. 6 and are deprotonated (COO^-) at pH 7[44] The scope of this study was to estimate the impact of the chromophore's charge on the H_2 production efficiency. We combined the photosensitizers with two cobaloxime-based catalysts (**CoPy** and **CoNMeim**) and used the following experimental conditions: 4×10^{-5} M of porphyrin, 4.9×10^{-4} M of the catalyst in a 1:1 $CH_3CN:H_2O$ solvent mixture of 5% (v/v) TEOA at pH 6, 7 and 8. We have no indication of catalyst decomposition or protonation of the axial ligand at these pH values.

The neutral zinc porphyrins **ZnTPyP**, **ZnTPP-[COOMe]$_4$**, **ZnTPP-[PO(OEt)$_2$]$_4$**, the positively charged tin chromophore **[Sn(OH)$_2$TMePyP$^+$]Cl$_4$** and negatively charged **ZnTPP-[COOH]$_4$**, **Sn(Cl$_2$)TPP-[COOH]$_4$** showed no activity with the two cobaloxime catalysts after 24 hours of irradiation. However, the positively charged zinc porphyrin **[ZnTMePyP$^+$]Cl$_4$** and the neutral tin porphyrins **Sn(OH)$_2$TPyP**, **Sn(Cl$_2$)TPP-[COOMe]$_4$** or **Sn(Cl$_2$)TPP-[PO(OEt)$_2$]$_4$** were photocatalytically active when combined with **CoPy**. The calculated turnover numbers (TONs) with respect to the photosensitizer were 320, ~10, 60 and 24 for **[ZnTMePyP$^+$]Cl$_4$**, **Sn(OH)$_2$TPyP**, **Sn(Cl$_2$)TPP-[COOMe]$_4$** or **Sn(Cl$_2$)TPP-[PO(OEt)$_2$]$_4$**, respectively. Under the same experimental conditions, **CoNMeim** was used instead of **CoPy** and the TONs of the photocatalytic H_2 production were significantly increased. The details are shown in Figure 5, the TON for **[ZnTMePyP$^+$]Cl$_4$** was

1135, 303 for **Sn(OH)$_2$TPyP**, 128 for **Sn(Cl$_2$)TPP-[COOMe]$_4$** and 48 for **Sn(Cl$_2$)TPP-[PO(OEt)$_2$]$_4$**. Table S3 lists the optimum photocatalytic conditions for all porphyrin photosensitizers. Overall, the positively charged zinc porphyrin (**[ZnTMePyP$^+$]Cl$_4$**) and the three neutral tin porphyrins (**Sn(OH)$_2$TPyP**, **Sn(Cl$_2$)TPP-[COOMe]$_4$** and **Sn(Cl$_2$)TPP-[PO(OEt)$_2$]$_4$**) were active towards H_2 evolution.

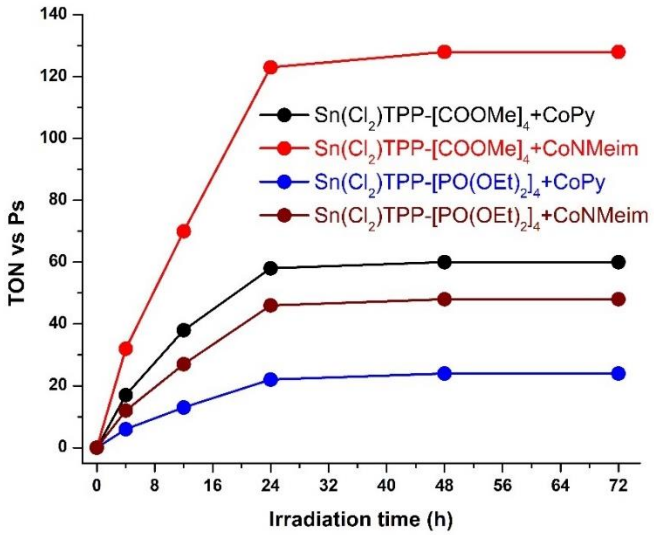

Figure 5. Plot of hydrogen production upon irradiation of solutions 1:1 CH_3CN:H_2O containing **Sn(Cl$_2$)TPP-[COOMe]$_4$** or **Sn(Cl$_2$)TPP-[PO(OEt)$_2$]$_4$** (4×10^{-5} M), **CoPy** or **CoNMeim** (4.9×10^{-4} M) and TEOA [5% (v/v)] at pH 7.

Additional studies have shown that light-driven hydrogen generation is strongly influenced by the proton concentration (pH). Thus, experiments with different pH values were carried out and only some traces of hydrogen were obtained at pH 6 and 8. These findings are consistent with results for related photocatalytic systems[16-18] in which the optimum pH value was close to the pKa value of the sacrificial electron donor, which is 7.9 for TEOA in aqueous solution. However, in the solution that we performed the photocatalytic experiments (1:1 CH_3CN:H_2O), the pKa value of TEOA is 7.[6] The optimum photocatalytic pH value for our systems was pH 7 which is consistent with this.

The performance of the photocatalytic hydrogen evolution system also depends on the catalyst and photosensitizer concentrations. In our previous work, **Sn(OH)$_2$TPyP** drove photocatalysis when combined with **CoPy** (TON~10).[18] We observed that hydrogen production was increased when the concentration of both the catalyst and the photosensitizer were increased (from 4.9 x 10^{-4} M to 9.8 x 10^{-4} M and 4 x 10^{-5} M to 8 x 10^{-5} M, respectively). Under 100 h of light irradiation, the above-mentioned photocatalytic system reached a maximum TON of 150. This increased hydrogen production is mainly attributed to the high stability of **CoPy** and in addition to the competition between the two main catalytic processes (reductive and oxidative). When **CoNMeim** was used as

the catalyst, the TON for photocatalytic hydrogen evolution increased significantly (TON = 303) using concentrations of 4×10^{-5} M for **Sn(OH)$_2$TPyP** and 4.9×10^{-4} M for **CoNMeim**. TEOA was used as the sacrificial electron donor [5 % (v/v)] and the photocatalytic activity lasted for 96 hours. When the concentration of both the catalyst and the photosensitizer were increased (red line, Figure 6), hydrogen production decreased considerably. As illustrated in Figure 6, when the concentration of **Sn(OH)$_2$TPyP** was increased to 8×10^{-5} M and **CoNMeim** was kept at 4.9×10^{-4} M we observed a maximum TON of 186 after 96 h of irradiation.

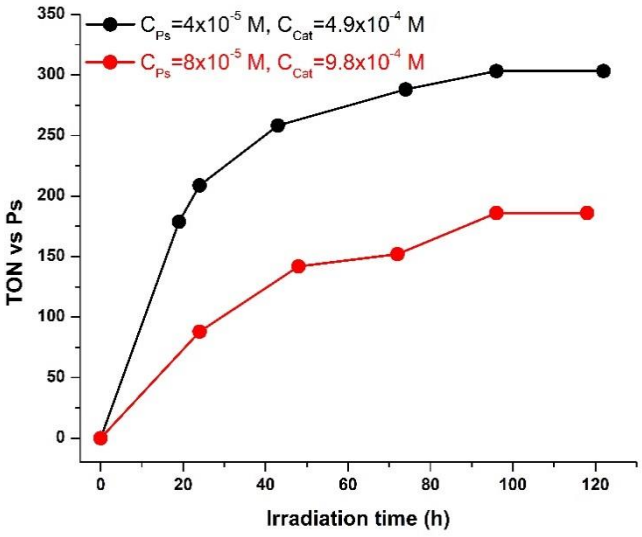

Figure 6. Plot of hydrogen production upon irradiation of solutions 1:1 CH_3CN:H_2O containing **Sn(OH)$_2$TPyP** and **CoNMeim** in different concentrations and **TEOA** [5% (v/v)] at pH 7.

Electrochemical properties

The redox potentials were significantly modified across the series of compounds examined here. Table 2 reports the redox potentials for the porphyrins in DMF solution, which were determined by cyclic voltammetry. In all cases,[36-42,45,46] the oxidation and reduction peaks were electrochemically reversible or quasi-reversible, allowing the formal redox potentials in the chosen supporting electrolyte to be determined. The first ground state oxidation potential ($E(Ps^+/Ps)$) and first ground state reduction potential $E(Ps/Ps^-)$ were used to estimate the excited state redox potentials of the triplet and singlet states (Table 2). The redox potentials of **CoNMeim** in CH_3CN:H_2O (1:1) were recorded by cyclic voltammetry (Figure S5), where we were able to detect two processes, in agreement with Panagiotopoulos *et al*[17]. The first one (-0.20 V vs. NHE), can be assigned to Co^{II}/Co^{III} process, while, the $Co^{I/II}$ wave lies at -0.55 V vs. NHE. The peaks were better resolved by recording differential pulse voltammetry (Figure S6) in the same solvent.[47-51] Similar to **CoNMeim**, the **CoPy** catalyst presents two reduction waves. The first one which is attributed to the $Co^{II/III}$

process can be observed at -0.43 V vs. NHE in CH_3CN or at -0.37 V vs. NHE in DMF. The second reduction is attributed to the $Co^{I/II}$ wave and lies at -0.88 V vs NHE in CH_3CN or at -0.76 V vs NHE in DMF.[51]

Table 2. Estimated energies and redox potentials for the singlet and triplet excited states of zinc and tin porphyrins

	E_{00} (^{1}Ps*) /eV	E_{00} (^{3}Ps*) /eV	E(Ps/Ps$^-$)	E(Ps$^+$/Ps)	E' (Ps$^+$/^{1}Ps*) /V	E' (1Ps*/Ps$^-$) /V	E' (Ps$^+$/^{3}Ps*) /V	E' (^{3}Ps*/Ps$^-$) /V
ZnTPyP[a] [37]	2.07	1.59	-0.65	1.04	-1.03	1.42	-0.55	0.94
[ZnTMePyP$^+$]Cl$_4$	2.01	1.63	-0.79	1.28	-0.73	1.22	-0.35	0.84
ZnTPP-[COOH]$_4$	2.06	1.60	-1.17	1.10	-0.96	0.89	-0.50	0.43
ZnTPP-[COOMe]$_4$	2.06	1.63	-1.16	1.09	-0.97	0.90	-0.54	0.47
ZnTPP-[PO(OEt)$_2$]$_4$	2.06	1.66	-1.32	1.14	-0.92	0.74	-0.52	0.34
Sn(OH)$_2$TPyP	2.08	1.66	-0.44	1.38	-0.70	1.64	-0.28	1.22
[Sn(OH)$_2$TMePyP$^+$]Cl$_4$[a] [42]	2.06	1.63	-0.3	1.69	-0.37	1.76	0.06	1.33
Sn(Cl$_2$)TPP-[COOH]$_4$[41]	2.07	1.63	-0.73	1.42	-0.65	1.34	-0.21	0.90
Sn(Cl$_2$)TPP-[COOMe]$_4$	2.06	1.66	-0.36	1.29	-0.77	1.70	-0.37	1.30
Sn(Cl$_2$)TPP-PO(OEt)$_2$]$_4$	2.06	1.65	-0.38	1.32	-0.74	1.68	-0.33	1.27

[a]Reported vs Fc/Fc$^+$ (+630 mV conversion to NHE)[45]; Data measured vs. Fc/Fc$^+$ in DMF converted to NHE by adding 720 mV.[52,53] E_{00} (^{1}Ps*) is the zero-zero energy transition of the singlet excited state in eV estimated from the intercept of the absorption and emission spectra, E_{00} (^{3}Ps*) is the zero-zero energy transition of the triplet excited state in eV which was found in literature for every porphyrin. First excited state oxidation potential (E' (Ps$^+$/Ps*)) and reduction potential (E' (Ps*/Ps$^-$)) of singlet and triplet state were calculated according to E'(Ps$^+$/Ps*) = $E_{ox} - E_{00}$ and E' (Ps*/Ps$^-$) =$E_{red} + E_{00}$.

Transient absorption measurements

Laser flash photolysis transient absorption measurements were performed to investigate the light-induced charge transfer dynamics of each of the porphyrin dyes in 1:1 CH_3CN:H_2O solution, to check for consistency with the hydrogen evolution measurements, both in the presence and in the absence of TEOA and the cobalt catalyst **CoNMeim**. The spectra are provided in Figures S7 to Figure S15 in the SI. For each porphyrin the singlet excited state (S1) decayed due to intersystem crossing to the lowest triplet state (T1), within the 4 ns laser pulse (Eq.1).

$$Ps + h\nu \rightarrow {}^1Ps^* \qquad \text{(Eq. 1)}$$

$$^1Ps^* \rightarrow {}^3Ps^* \qquad \text{(Eq. 2)}$$

For each porphyrin, the spectral features observed at early delay times were characteristic of a T1 excited state, with lifetime $\tau(^3Ps^*)$ containing a broad positive band, with a maximum at around 450-500 nm, which extended to about 700 nm, and an overlapping negative feature at around 600 nm, due to the bleach of the Q-bands. The oxidised state of the zinc tetraphenyl porphyrins is weakly absorbing in the visible region, as confirmed by recording the absorption spectrum of **ZnTPyP** upon chemical oxidation with $NOBF_4$ (see Figure S16). As it was difficult to distinguish between the differential absorption spectrum of **^{3}ZnPs*** and **ZnPs$^{\cdot+}$**, **τ** for the formation of oxidised state, after the addition of **CoNMeim**, was inferred from the quenching of **^{3}ZnPs*** (**τ**(*^{3}Ps + **CoNMeim**)).

Previous studies using ns resolution transient absorption spectroscopy showed, firstly, that **[ZnTMePyP$^+$]Cl$_4$** decomposes on excitation in the presence of TEOA, implying that probably the TEOA generates the chlorin.[16,27] Secondly, it was reported that the addition of the cobalt catalyst oxidatively quenches the porphyrin T1 state (Eq. 3), leading to a decrease in the lifetime of ***[ZnTMePyP$^+$]Cl$_4$**, from **τ**(***[ZnTMePyP$^+$]Cl$_4$**) >100 μs to **τ**(***[ZnTMePyP$^+$]Cl$_4$**) ~2 μs.[16] This is consistent with the participation of porphyrin excited state in the hydrogen production pathway B in Scheme 1. Our experiments were in agreement with this analysis, and we found that the cobalt catalyst quenched ***[ZnTMePyP$^+$]Cl$_4$** (see Table 3). Under a nitrogen purged atmosphere, the amplitude weighted lifetime of ***[ZnTMePyP$^+$]Cl$_4$** decreased more than ten-fold from **τ**(*^{3}**[ZnTMePyP$^+$]Cl$_4$**) = 85 μs to **τ**(*^{3}**[ZnTMePyP$^+$]Cl$_4$** + **CoNMeim**) =** 4 μs both in the absence and presence of TEOA.

For zinc porphyrins **ZnTPP-[PO(OEt)$_2$]$_4$** (Figure S11 b), **ZnTPP-[COOMe]$_4$** (Figure S10 b), **ZnTPP-[COOH]$_4$** (Figure S12 b), **ZnTPyP** (Figure S13 b), the shape of the transient spectra of *ZnPs in the presence and in the absence of TEOA was unchanged, both spectra contain transient bands around 460 nm and the lifetimes of these bands was similar to those obtained in the presence of ZnPs* only. This was expected as from Table 2, it can be seen that the formation of **ZnPs$^{\cdot-}$** from **^{*3}ZnPs** is thermodynamically unfavorable for these porphyrins. A slight increase in lifetime was observed in some cases, which can be attributed to the coordination of ZnPs with TEOA. [24,48,49] The addition of **CoNMeim** to these zinc porphyrins had a slight effect (**ZnTPP-[PO(OEt)$_2$]$_4$**, **ZnTPyP** and **ZnTPP-[COOH]$_4$**) or no effect (**ZnTPP-[COOMe]$_4$**) on **τ(^{*3}ZnPs)** (Table 3). This demonstrates that in these cases, a mild reaction with the catalyst occurred.

CoNMeim was observed to quench the ^{3}Ps* of **Sn(Cl$_2$)TPP-[COOMe]$_4$** (Figure S8) and **Sn(OH)$_2$TPyP** (Figure S9), leading to shorter lifetimes in the presence of the catalyst (Table 3). **SnPs$^{\cdot+}$**, formed after the addition of the catalyst, was difficult to distinguish from **^{3}SnPs*** (see Figure S16), so the formation of oxidised state was estimated from the difference in **^{3}SnPs*** lifetime after **CoNMeim** was added. For **Sn(Cl$_2$)TPP-[COOMe]$_4$** in the presence of **CoNMeim**, two lifetimes at 450 nm were detected, the shorter component is associated with the quenching of the excited state, **τ(*Sn(Cl$_2$)TPP-[COOMe]$_4$ + CoNMeim)** = 2 μs, and the longer component is the lifetime of the oxidised product, **τ(Sn(Cl$_2$)TPP-[COOMe]$_4^{\cdot+}$)$_3$** = 10 μs. For these porphyrins, it was possible to observe the reduced state (SnPs$^{\cdot-}$), formed in the presence of TEOA (Eq. 4). For tin porphyrins, the transient spectrum of SnPs$^{\cdot-}$ contained a peak at 450 nm, which was blue-shifted with respect to ^{3}SnPs*. For both **Sn(Cl$_2$)TPP-[COOMe]$_4$** and **Sn(OH)$_2$TPyP** in the presence of TEOA (Figure S8b and Figure S9b), the transient absorption at 450 nm decayed biexponentially. The shorter lifetime with respect to **τ(*Sn(OH)$_2$TPyP) =** 78 μs and **τ(*Sn(Cl$_2$)TPP-[COOMe]$_4$) =** 70 μs, has been assigned to triplet state, which was slightly quenched, and the longer lived species, to the reduced state, **τ(Sn(OH)$_2$TPyP$^{\cdot-}$)** = 200 μs and **τ(Sn(Cl$_2$)TPP-[COOMe]$_4^{\cdot-}$)** = 150 μs.

Both **Sn(Cl$_2$)TPP-[COOH]$_4$** and **[Sn(OH)$_2$TMePyP$^+$]Cl$_4$** were found to be pretty unstable in the presence of TEOA, forming the chlorin. At the same time, ***Sn(Cl$_2$)TPP-[COOH]$_4$** and ***[Sn(OH)$_2$TMePyP$^+$]Cl$_4$** were not quenched in the presence of **CoNMeim** (**τ**(*Sn(Cl$_2$)TPP-[COOH]$_4$ + CoNMeim) = 180 μs, **τ**(*[Sn(OH)$_2$TMePyP$^+$]Cl$_4$ + CoNMeim) = 192 μs). Transient absorption studies were not carried out for **Sn(Cl$_2$)TPP-[PO(OEt)$_2$]$_4$** as it was not sufficiently soluble in the solvents employed.

Table 3. Lifetime **τ** of porphyrins alone and in the presence of **CoNMeim** and/or TEOA.

Photosensitizers	τ(*^{3}Ps) (μs)[a]	τ(Ps + CoNMeim) (μs)[b]	τ (Ps + TEOA) (μs)[c]	τ (Ps + TEOA + CoNMeim) (μs)[d]
ZnTPyP	150 ± 5	135± 6	148±4	134±6
Sn(OH)$_2$TPyP	78 ± 6	7 ± 2	24 ± 4 (τ_1), 200 ± 8 (τ_2) (A_1 = 0.3, A_2 = 0.7)	10 ± 4
[ZnTMePyP$^+$]Cl$_4$	85 ± 3	4 ± 1	-[e]	4 ± 0.5
[Sn(OH)$_2$TMePyP$^+$]Cl$_4$	190 ± 9	192 ± 5	-[e]	-[e]
ZnTPP-[COOH]$_4$	278 ± 6	264 ± 5	280 ± 4	262 ± 9
Sn(Cl$_2$)TPP-[COOH]$_4$	182 ± 7	175 ± 5	-[e]	-[e]
ZnTPP-[COOMe]$_4$	149 ± 4	148 ± 6	150 ± 5	146 ± 9
Sn(Cl$_2$)TPP-[COOMe]$_4$	70 ± 4	2 ± 0.2, 10 ± 4 (A_1 = 0.65, A_2 = 0.35)	20 ± 2 (τ_1), 150 ± 8 (τ_2) (A_1 = 0.2, A_2 = 0.8)	7 ± 3
ZnTPP-[PO(OEt)$_2$]$_4$	70 ± 5	57 ± 6	69 ± 6	60 ± 6
Sn(Cl$_2$)TPP-[PO(OEt)$_2$]$_4$	-[f]	-[f]	-[f]	-[f]

[a]5 x 10^{-5} M porphyrin in 1:1 $CH_3CN:H_2O$; [b]5 x 10^{-5} M porphyrin + 10 equivalents **CoNMeim** in MeCN:H_2O (1:1); [c]5 x 10^{-5} M porphyrin + 5% TEOA in 1:1 $CH_3CN:H_2O$; [d]5 x 10^{-5} M porphyrin + 5% TEOA + 10 equivalents **CoNMeim** in 1:1 $CH_3CN:H_2O$; [e]decomposes in the presence of TEOA and no reaction with **CoNMeim**; [f]insufficiently soluble in the solvent employed (MeCN:H_2O 1:1).

DISCUSSION

The reduction of Co^{III} to Co^{II}, the first step of the catalytic cycle, may occur either by direct electron transfer from the porphyrin excited state, forming the oxidised porphyrin $Ps^{\cdot+}$, with a lifetime **τ**($Ps^{\cdot+}$), (Eq. 3) or by reductive quenching of excited state by TEOA (Eq. 4), forming the reduced porphyrin, $Ps^{\cdot-}$, with a lifetime **τ**($Ps^{\cdot-}$), followed by electron transfer between $Ps^{\cdot-}$ and Co^{III} (Eq. 6). The byproduct $TEOA^+$ is a very strong reductant and can transfer its electron to a further excited or ground state Ps.[54]

$$Ps^* + Co^{III} \rightarrow Ps^{\cdot+} + Co^{II} \quad \text{(Eq. 3)}$$

$$Ps^* + TEOA \rightarrow Ps^{\cdot-} + TEOA^+ \quad \text{(Eq. 4)}$$

$$Ps^{\cdot+} + TEOA \rightarrow Ps + TEOA^+ \quad \text{(Eq. 5)}$$

$$Ps^{\cdot-} + Co^{III} \rightarrow Ps + Co^{II} \quad \text{(Eq. 6)}$$

$$Co^{II} + 2e^- + 2H^+ \rightarrow Co^{III} + H_2 \quad \text{(Eq. 7)}$$

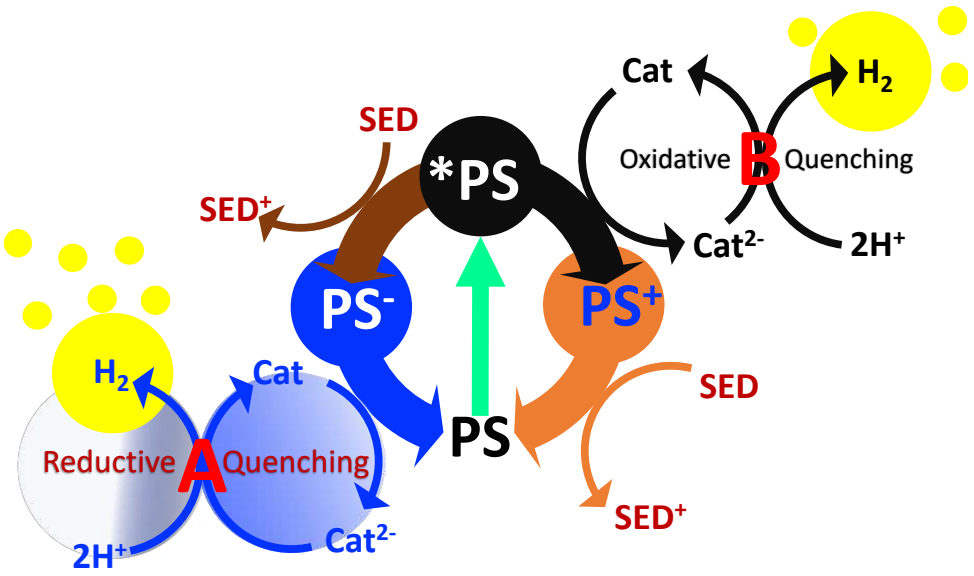

Scheme 1: Schematic representation of the two main mechanisms leading to **CoNMeim** reduction and hydrogen generation. For clarity reasons the following abbreviations are used: Ps=zinc/tin porphyrins, and Cat = **CoNMeim**

The redox potential of TEOA (1.07 V vs NHE)[55] is appropriate to reductively quench the singlet excited state (^{1}Ps*) of **ZnTPyP**, **[ZnTMePyP$^+$]Cl$_4$** and all of the tin porphyrins (E' (^{1}Ps*/Ps$^-$) > 1.07 V). It is also thermodynamically feasible for the ^{1}Ps* of all the porphyrins investigated in this study (except **[Sn(OH)$_2$TMePyP$^+$]Cl$_4$**) to be oxidatively quenched by both the Co^{III} and Co^{II} species. It is unlikely that quenching occurs from ^{1}Ps* in these cases, however, since the lifetimes of the porphyrins in the presence of the catalyst and sacrificial electron donor are much longer than the lifetime of the singlet excited state of the porphyrin, which is only a couple of ns. Furthermore, only a few porphyrins were quenched, either oxidatively or reductively, despite there being sufficient driving force for the electron transfer reaction. Instead, it is more likely that the reactions take place from the less energetic ^{3}Ps*.

The redox potentials of the triplet excited state of the ZnPs are insufficient to oxidize TEOA efficiently, whereas it is thermodynamically favourable for most of the ^{3}SnPs* (except **Sn(Cl$_2$)TPP-[COOH]$_4$**) to be quenched by TEOA. If reductive quenching occurred before electron transfer to the catalyst (pathway A), it would be thermodynamically possible for all the porphyrins to reduce the catalyst from Co^{III} to Co^{II}. E'(Ps/Ps$^-$) is more negative than E'(Co^{II}/Co^{I}) for all the zinc porphyrins and **Sn(Cl$_2$)TPP-[COOH]$_4$**. Therefore, if the first step is the reduction of the ^{3}SnPs* by the sacrificial electron donor, we would not expect **[ZnTMePyP$^+$]Cl$_4$** or the tin porphyrins to drive the photocatalysis, which is not consistent with the observations described above.

The ^{3}Ps* oxidation potential is sufficiently negative for of all the zinc porphyrins to reduce **CoNMeim** from Co^{III} to Co^{II}. From the tin porphyrins, however, only **Sn(OH)$_2$TPyP**, **Sn(Cl$_2$)TPP-[COOMe]$_4$** and **Sn(Cl$_2$)TPP-PO(OEt)$_2$]$_4$** have sufficient reducing power in the long lived ^{3}Ps* to reduce the Co^{III} (except) and the ^{3}Ps* oxidation potential is not sufficiently negative for any of the porphyrins to reduce **CoNMeim** from Co^{II} to Co^{I}. *E'*(Ps^+/Ps) is very close to *E*'($TEOA^+$/TEOA) for four of the zinc porphyrins, which means that should oxidative quenching by the catalyst occur first, these porphyrins would not be efficiently re-reduced. *E'*(Ps^+/Ps) for **[ZnTMePyP$^+$]Cl$_4$** and all the tin porphyrins lies more positive than *E*'($TEOA^+$/TEOA), so it is likely that these would be re-reduced by TEOA following oxidative quenching by **CoNMeim**. This pathway is consistent with the photocatalysis results. The porphyrins which generated hydrogen were all observed to be oxidatively quenched by **CoNMeim** in the transient absorption spectroscopy experiments. For the zinc porphyrins which could be oxidatively quenched by the catalyst, only **[ZnTMePyP$^+$]Cl$_4$** can be re-reduced by TEOA, which is consistent with this being the only zinc porphyrin to drive photocatalysis in our experiments. The lifetimes for the porphyrin in the presence of catalyst and TEOA were similar to the lifetimes for the porphyrin and catalyst only, which is also consistent with pathway B. The advantage of pathway B over pathway A (which is thermodynamically feasible for **Sn(Cl$_2$)TPP-[COOMe]$_4$**, **Sn(OH)$_2$TPyP** and **[ZnTMePyP$^+$]Cl$_4$**) is that the reduced porphyrin is not present in large concentrations, which could lead to the formation of the chlorin and subsequent decomposition of the PS. The subsequent step in the catalytic reaction, which we have not investigated here, is the second reduction of the catalyst. The ^{3}Ps* oxidation potential is not sufficiently negative to reduce the catalyst to Co^1. The oxidation potential of the TEOA-derived alkyl radical / iminium cation is *ca.* –790 mV vs. NHE in MeCN,[56] which is sufficient to provide the second electron to the **CoNMeim** catalyst.

CONCLUSIONS

In conclusion, the synthesis of zinc and tin porphyrins as light harvesting units and cobaloxime complexes as catalysts towards light-driven hydrogen evolution is presented. Moreover, the influence of the charge of the *para*-substituents of meso-phenyl groups of the porphyrin in photo-induced performance is examined. The thorough studies performed in this work illustrated that the positively charged zinc porphyrin **[ZnTMePyP$^+$]Cl$_4$** and the neutral tin porphyrin derivatives **Sn(OH)$_2$TPyP**, **Sn(Cl$_2$)TPP-[COOMe]$_4$** and **Sn(Cl$_2$)TPP-[PO(OEt)$_2$]$_4$** are photocatalitically active, reaching maximum TONs of 1135, 303, 128 and 48, respectively. Furthermore, photophysical and electrochemical investigation was conducted in order to determine the mechanism of the photocatalytic hydrogen production using charged or neutral porphyrins as light

harvesting units. Overall, we have shown that the photocatalysis is most likely to proceed via oxidative quenching of the porphyrin sensitizer, leading to the reduced catalyst. The photosensitizer is regenerated subsequently by the oxidation of TEOA. Careful examination over the ground and excited state redox properties enabled the appropriate functionalazation of the porphyrin periphery; allowing the fine tuning of the charge-transfer dynamics and consequently the photocatalytic activity.

EXPERIMENTAL SECTION

General

Reagents and solvents were purchased as reagent grade from usual commercial sources and used without further purification, unless otherwise stated. Thin layer chromatography was performed on silica gel 60 F_{254} plates, while chromatographic separations were carried out using silica gel 60, SDS, 70–230 mesh ASTM.

^{1}H NMR and ^{13}C NMR spectra were recorded on Bruker AMX-500 MHz and Bruker DPX-300 MHz spectrometers, as solutions in deuterated solvents by using the solvent peak as the internal standard. High-resolution mass spectra were recorded on a Bruker ultrafleXtreme MALDI-TOF/TOF spectrometer, using trans-2-[3-(4-tert-butylphenyl)-2-methyl-2-propenylidene]malononitrile as matrix.

X-ray crystallography.

A single-crystal of compound **Sn(Cl$_2$)TPP-[COOMe]$_4$·2**CH_2Cl_2, suitable for X-ray crystallographic analysis, was protected with paratone-N and mounted for data collection on a STOE IPDS II diffractometer equipped with a Mo-Kα sealed-tube X-ray source (λ = 0.71073 Å, graphite monochromated) and an image plate detector. Data collection, data reduction, integration, and cell parameters determination were carried out using the STOE X-AREA package software,[57] while a numerical absorption correction was also applied using the STOE X-RED and X-SHAPE software packages.[58,59] The structure was solved using direct methods, implemented in SHELXS-2014,[60,61] and refined using SHELXL-2014.[62] All non-hydrogen atoms were successfully refined using anisotropic displacement parameters. A plot of the molecular structure of the compound was obtained by using the program Mercury.[63]

Photophysical Measurements

UV-Vis absorption spectra were measured on a Shimadzu UV-1700 spectrophotometer using 10 mm path-length cuvettes.

Nanosecond transient measurements were performed with a custom laser spectrometer comprised of a Brillian Quantel laser with frequency doubled (532 nm, 330 mJ) or tripled (355 nm, 160 mJ) option, an Applied Photophysics xenon light source including a mod. 720 150 W lamp

housing, a mod. 620 power controlled lamp supply and a mod. 03- 102 arc lamp pulser. Laser excitation was provided at 90° with respect to the white light probe beam. Light transmitted by the sample was focused onto the entrance slit of a SpectraKinetic monochromator (Applied photophysics). Kinetic traces were processed by means of a Agilent digital oscilloscope. A typical pulse energy of 2 mJ cm^{-2} was used.

Electrochemistry

Electrochemical studies were carried out using an IviumStat potentiostat controlled using IviumSoft. Redox potentials were determined using cyclic voltammetry. Electrochemistry was performed under a nitrogen atmosphere, using a three-electrode setup, in a single compartment cell. A glassy carbon working electrode, a Pt wire secondary electrode and a Ag/Ag^+ (0.01 M $AgNO_3$ in acetonitrile) reference electrode were used. The redox potential of **Sn(Cl$_2$)TPP-[COOMe]$_4$** was measured with a 1 mM analyte concentration in anhydrous acetonitrile that had been purged with nitrogen, with 0.1M $TBAPF_6$ supporting electrolyte. The redox potential of **CoNMeim** was measured under the same conditions but with a 50:50 mixture of water:acetonitrile that had been purged with nitrogen, with 0.1 M $LiClO_4$ supporting electrolyte. The reference electrodes were calibrated against ferrocene.

Photocatalytic hydrogen evolution experiments

For photoinduced hydrogen evolution, each sample was prepared in a 42 mL glass vial with silicone septum. Prior to sample preparation, an aqueous solution of TEOA (10% vol) was adjusted to pH 7 using conc. HCl. The components were then dissolved in 10 ml of a 1:1 (v/v) mixture of acetonitrile and aqueous TEOA (10%) solution. The mixture was degassed for 10 minutes using nitrogen at room temperature. Then, the samples were sealed and irradiated with a white LED ring (power of 40 W, color temperature of 6400 K and lumen of 3800 LM, Figure S15). The amounts of hydrogen evolved were determined by gas chromatography (external standard technique) using a Shimadzu GC 2010 plus chromatograph with a TCD detector and a molecular sieve 5 Å column (30 m - 0.53 mm). 100 μL were taken from the headspace and injected immediately into the GC. In all cases, the reported TON (with respect to the porphyrin) is the average of three independent experiments. Control experiments were performed under the same experimental conditions. We performed various experiments by removing only the catalyst or the photosensitizer from the hydrogen generating system, but we did not detect any H_2 production. In addition, mercury poisoning experiments were performed, in order to examine the possible formation of metallic nanoparticles or colloids during the hydrogen evolution process. In these studies, an excess of mercury (ca. 40 equiv.) was added to the hydrogen evolution solutions but H_2 production was detected at the same levels as in the regular photocalatytic experiments (absence of mercury).

Synthesis

The catalysts **CoPy** and **CoNMeim** were prepared according to the literature.[17] In addition, the Zn (**ZnTPyP**, **ZnTPP-[COOMe]$_4$**, **ZnTPP-[PO(OEt)$_2$]$_4$**, **[ZnTMePyP$^+$]Cl$_4$** and negatively **ZnTPP-[COOH]$_4$**)[36-39] and the Sn porphyrin derivatives (**Sn(OH)$_2$TPyP**, **Sn(Cl$_2$)TPP-[COOMe]$_4$**, **Sn(Cl$_2$)TPP-[PO(OEt)$_2$]$_4$**), **[Sn(OH)$_2$TMePyP$^+$]Cl$_4$** and **Sn(Cl$_2$)TPP-[COOH]$_4$**)[18,40-43] were synthesized as previously reported.

Diethyl–4–formylphenylphosphonate. 4-bromobenzaldehyde (500 mg, 2.70 mmol) was added in a 100 mL two-necked bottom flask. To this solution, dry toluene (4 mL), dry Et_3N (4 mL) and diethylphosphite (0.4 mL, 6 mmol) were added and purged with Ar gas for 2 min, followed by addition of $Pd(PPh_3)_4$ (155 mg, 0.135 mmol). The reaction mixture was heated to 90 ºC for 24 h under Ar atmosphere. The reaction mixture was cooled down to room temperature and the solvent was evaporated to dryness under vacuum, re-dissolved in $CHCl_3$ (35 mL), washed with distilled water (3 × 50 mL), followed by brine solution (50 mL), and finally dried over with Na_2SO_4. The crude product was purified on a silica column chromatography using $CHCl_3$: EtOAc (70:30, v/v) as the eluent. After distillation under vacuum **diethyl–4–formylphenylphosphonate** was obtained as a colorless liquid. Yield: 300 mg (47%). ^{1}H NMR (300 MHz, $CDCl_3$): δ 10.09 (s, 1H, CHO), 7.98(m, 4H, ph-H), 4.15(m, 4H, -CH_2), 1.34(t, *J*= 7.1Hz, 6H, -CH_3) ppm. [64]

5,10,15,20-tetrakis-(4-di-ethyl-phosphonate-phenyl) porphyrin **(H$_2$TPP-[PO(OEt)$_2$]$_4$).** A solution of diethyl–4–formylphenylphosphonate (280 mg, 1.18 mmol) and pyrrole (0.080 mL, 1.15 mmol) in 10 mL of propionic acid was refluxed at 150 ºC in a flask protected from light for 1.5 h. The reaction mixture was evaporated to dryness, and purified by column chromatography on neutral alumina eluting with a mixture of CH_2Cl_2 : MeOH (99:1, v/v) to obtain the **H$_2$TPP-[PO(OEt)$_2$]$_4$** as a dark purple solid. Yield: 92.4 mg (28%).^{1}H NMR (500 MHz, $CDCl_3$): δ 8.83 (s, 8H, pyr), 8.33 (m, 8H, o-ph), 8.22 (m, 8H, m-ph), 4.38 (m, 16H, -OCH_2), 1.52 (t, *J*= 7.3Hz, 24H, -CH_3), -2.83 (s, 2H, -NH) ppm. HRMS (MALDI-TOF): m/z calcd. for $C_{60}H_{66}N_4O_{12}P_4$ $[M]^+$ 1158.3628, found. 1158.3633, UV/Vis (CH_2Cl_2): λ_{max}, nm: 419, 515, 549, 590, 646. [64,65]

trans-dichloro[5,10,15,20-tetrakis-(4-di-ethyl-phosphonate-phenyl) porphyrinato] tin(IV) **(Sn(Cl$_2$)TPP-[PO(OEt)$_2$]$_4$)**. In a round bottom flask porphyrin **H$_2$TPP-[PO(OEt)$_2$]$_4$** (188 mg, 0.162 mmol), $SnCl_2$ (307 mg, 1.62 mmol), pyridine (30 mL) were added and refluxed for 9 hours. The solvent was evaporated to dryness under vacuum. The solid was dissolved in CH_2Cl_2 and was filtered with celite to obtain the **Sn(Cl$_2$)TPP-[PO(OEt)$_2$]$_4$** as a dark purple solid. Yield: 108 mg (50%). Due to solubility reasons we were unable to record NMR spectrums for **Sn(Cl$_2$)TPP-**

[PO(OEt)$_2$]$_4$. HRMS (MALDI-TOF): m/z calcd. for $C_{60}H_{64}Cl_2N_4O_{12}P_4Sn$ $[M\text{-}Cl]^+$ 1311.2182, found 1311.2165, UV/Vis (CH_2Cl_2) λ_{max}, nm: 428, 561, 600.

ASSOCIATED CONTENT

Supporting Information

ACKNOWLEDGMENTS

EAG, GC, JK and EB thank The North East Centre for Energy Materials EP/R021503/1. The raw data for the transient spectroscopy and electrochemistry are available free of charge at https://data.ncl.ac.uk/. This research was funded by the General Secretariat for Research and Technology (GSRT) and Hellenic Foundation for Research and Innovation (HFRI) (project code: 508). This research has also been co-financed by the European Union and Greek national funds through the Operational Program Competitiveness, Entrepreneurship, and Innovation, under the call RESEARCH – CREATE – INNOVATE (project code: T1EDK-01504). In addition, this research has been co-financed by the European Union and Greek national funds through the Regional Operational Program "Crete 2014-2020", project code OPS: 5029187. Moreover, the European Commission's Seventh Framework Program (FP7/2007-2013) under grant agreement no. 229927 (FP7-REGPOT-2008-1, Project BIO-SOLENUTI) and the Special Research Account of the University of Crete are gratefully acknowledged for the financial support of this research.

REFERENCES

(1) Hosseini, S. E.; Wahid, M. A. Hydrogen production from renewable and sustainable energy resources: Promising green energy carrier for clean development. *Renewable & Sustainable Energy Reviews* **2016**, *57*, 850-866.

(2) Hosenuzzaman, M.; Rahim, N. A.; Selvaraj, J.; Hasanuzzaman, M.; Malek, A. B. M. A.; Nahar, A. Global prospects, progress, policies, and environmental impact of solar photovoltaic power generation. *Renewable & Sustainable Energy Reviews* **2015**, *41*, 284-297.

(3) Service, R. F. Solar energy - Is it time to shoot for the Sun? *Science* **2005**, *309*, 548-551.

(4) Lewis, N. S.; Nocera, D. G. Powering the planet: Chemical challenges in solar energy utilization. *Proceedings of the National Academy of Sciences of the United States of America* **2006**, *103*, 15729-15735.

(5) Andreiadis, E. S.; Chavarot-Kerlidou, M.; Fontecave, M.; Artero, V. Artificial Photosynthesis: From Molecular Catalysts for Light-driven Water Splitting to Photoelectrochemical Cells. *Photochemistry and Photobiology* **2011**, *87*, 946-964.

(6) Pellegrin, Y.; Odobel, F. Sacrificial electron donor reagents for solar fuel production. *Cr Chim* **2017**, *20*, 283-295.

(7) Lo, W. K. C.; Castillo, C. E.; Gueret, R.; Fortage, J.; Rebarz, M.; Sliwa, M.; Thomas, F.; McAdam, C. J.; Jameson, G. B.; McMorran, D. A.; Crowley, J. D.; Collomb, M. N.; Blackman, A. G. Synthesis,

Characterization, and Photocatalytic H-2-Evolving Activity of a Family of [Co(N4Py)(X)](n+) Complexes in Aqueous Solution. *Inorganic Chemistry* **2016**, *55*, 4564-4581.

(8) Khnayzer, R. S.; Thoi, V. S.; Nippe, M.; King, A. E.; Jurss, J. W.; El Roz, K. A.; Long, J. R.; Chang, C. J.; Castellano, F. N. Towards a comprehensive understanding of visible-light photogeneration of hydrogen from water using cobalt(II) polypyridyl catalysts. *Energy & Environmental Science* **2014**, *7*, 1477-1488.

(9) Goldsmith, J. I.; Hudson, W. R.; Lowry, M. S.; Anderson, T. H.; Bernhard, S. Discovery and high-throughput screening of heteroleptic iridium complexes for photoinduced hydrogen production. *J Am Chem Soc* **2005**, *127*, 7502-7510.

(10) Probst, B.; Guttentag, M.; Rodenberg, A.; Hamm, P.; Alberto, R. Photocatalytic H-2 Production from Water with Rhenium and Cobalt Complexes. *Inorg Chem* **2011**, *50*, 3404-3412.

(11) Probst, B.; Rodenberg, A.; Guttentag, M.; Hamm, P.; Alberto, R. A Highly Stable Rhenium-Cobalt System for Photocatalytic H-2 Production: Unraveling the Performance-Limiting Steps. *Inorg Chem* **2010**, *49*, 6453-6460.

(12) Probst, B.; Kolano, C.; Hamm, P.; Alberto, R. An Efficient Homogeneous Intermolecular Rhenium-Based Photocatalytic System for the Production of H-2. *Inorg Chem* **2009**, *48*, 1836-1843.

(13) Du, P. W.; Schneider, J.; Jarosz, P.; Eisenberg, R. Photocatalytic generation of hydrogen from water using a platinum(II) terpyridyl acetylide chromophore. *J Am Chem Soc* **2006**, *128*, 7726-7727.

(14) Li, T. T.; Chen, Y.; Fu, W. F. Photocatalytic H-2 production from water based on platinum(II) Schiff base sensitizers and a molecular cobalt catalyst. *Catal Commun* **2014**, *45*, 91-94.

(15) Du, P. W.; Schneider, J.; Jarosz, P.; Zhang, J.; Brennessel, W. W.; Eisenberg, R. Photoinduced electron transfer in platinum(II) terpyridyl acetylide chromophores: Reductive and oxidative quenching and hydrogen production. *J Phys Chem B* **2007**, *111*, 6887-6894.

(16) Lazarides, T.; Delor, M.; Sazanovich, I. V.; McCormick, T. M.; Georgakaki, I.; Charalambidis, G.; Weinstein, J. A.; Coutsolelos, A. G. Photocatalytic hydrogen production from a noble metal free system based on a water soluble porphyrin derivative and a cobaloxime catalyst. *Chemical Communications* **2014**, *50*, 521-523.

(17) Panagiotopoulos, A.; Ladomenou, K.; Sun, D. Y.; Artero, V.; Coutsolelos, A. G. Photochemical hydrogen production and cobaloximes: the influence of the cobalt axial N-ligand on the system stability. *Dalton Transactions* **2016**, *45*, 6732-6738.

(18) Landrou, G.; Panagiotopoulos, A. A.; Ladomenou, K.; Coutsolelos, A. G. Photochemical hydrogen evolution using Sn-porphyrin as photosensitizer and a series of Cobaloximes as catalysts. *Journal of Porphyrins and Phthalocyanines* **2016**, *20*, 534-541.

(19) Queyriaux, N.; Giannoudis, E.; Windle, C. D.; Roy, S.; Pecaut, J.; Coutsolelos, A. G.; Artero, V.; Chavarot-Kerlidou, M. A noble metal-free photocatalytic system based on a novel cobalt tetrapyridyl catalyst for hydrogen production in fully aqueous medium. *Sustainable Energy & Fuels* **2018**, *2*, 553-557.

(20) Nikoloudakis, E.; Karikis, K.; Han, J. J.; Kokotidou, C.; Charisiadis, A.; Folias, F.; Douvas, A. M.; Mitraki, A.; Charalambidis, G.; Yan, X. H.; Coutsolelos, A. G. A self-assembly study of PNA-porphyrin and PNA-BODIPY hybrids in mixed solvent systems. *Nanoscale* **2019**, *11*, 3557-3566.

(21) Salzl, S.; Ertl, M.; Knor, G. Evidence for photosensitised hydrogen production from water in the absence of precious metals, redox-mediators and co-catalysts. *Physical Chemistry Chemical Physics* **2017**, *19*, 8141-8147.

(22) Yuan, Y. J.; Tu, J. R.; Ye, Z. J.; Lu, H. W.; Ji, Z. G.; Hu, B.; Li, Y. H.; Cao, D. P.; Yu, Z. T.; Zou, Z. G. Visible-light-driven hydrogen production from water in a noble-metal-free system catalyzed by zinc porphyrin sensitized MoS2/ZnO. *Dyes and Pigments* **2015**, *123*, 285-292.

(23) Peuntinger, K.; Lazarides, T.; Dafnomili, D.; Charalambidis, G.; Landrou, G.; Kahnt, A.; Sabatini, R. P.; McCamant, D. W.; Gryko, D. T.; Coutsolelos, A. G.; Guldi, D. M. Photoinduced Charge Transfer in Porphyrin-Cobaloxime and Corrole-Cobaloxime Hybrids. *Journal of Physical Chemistry C* **2013**, *117*, 1647-1655.

(24) Zhang, P.; Wang, M.; Li, C. X.; Li, X. Q.; Dong, J. F.; Sun, L. C. Photochemical H-2 production with noble-metal-free molecular devices comprising a porphyrin photosensitizer and a cobaloxime catalyst. *Chemical Communications* **2010**, *46*, 8806-8808.

(25) Zhang, P.; Wang, M.; Li, X. Q.; Cui, H. G.; Dong, J. F.; Sun, L. C. Photochemical hydrogen production with molecular devices comprising a zinc porphyrin and a cobaloxime catalyst. *Science China-Chemistry* **2012**, *55*, 1274-1282.

(26) Ladomenou, K.; Natali, M.; Iengo, E.; Charalampidis, G.; Scandola, F.; Coutsolelos, A. G. Photochemical hydrogen generation with porphyrin-based systems. *Coordination Chemistry Reviews* **2015**, *304*, 38-54.

(27) Harriman, A.; Porter, G.; Richoux, M. C. Photosensitized Reduction of Water to Hydrogen Using Water-Soluble Zinc Porphyrins. *Journal of the Chemical Society-Faraday Transactions Ii* **1981**, *77*, 833-844.

(28) Kruger, W.; Fuhrhop, J. H. Evolution of Hydrogen from Photochemically Reduced Water-Soluble Tin(Iv)-Porphyrins. *Angewandte Chemie-International Edition in English* **1982**, *21*, 131-131.

(29) Arnold, D. P.; Blok, J. The coordination chemistry of tin porphyrin complexes. *Coordination Chemistry Reviews* **2004**, *248*, 299-319.

(30) Koposova, E.; Liu, X.; Pendin, A.; Thiele, B.; Shumilova, G.; Ermolenko, Y.; Offenhausser, A.; Mourzina, Y. Influence of Meso-Substitution of the Porphyrin Ring on Enhanced Hydrogen Evolution in a Photochemical System. *Journal of Physical Chemistry C* **2016**, *120*, 13873-13890.

(31) Natali, M.; Luisa, A.; Lengo, E.; Scandola, F. Efficient photocatalytic hydrogen generation from water by a cationic cobalt(II) porphyrin. *Chem Commun* **2014**, *50*, 1842-1844.

(32) Varma, S.; Castillo, C. E.; Stoll, T.; Fortage, J.; Blackman, A. G.; Molton, F.; Deronzier, A.; Collomb, M. N. Efficient photocatalytic hydrogen production in water using a cobalt(III) tetraaza-macrocyclic catalyst: electrochemical generation of the low-valent Co(I) species and its reactivity toward proton reduction. *Phys Chem Chem Phys* **2013**, *15*, 17544-17552.

(33) Zhiji, H.; R., M. W.; Min-Sik, E.; L., H. P.; Richard, E. A Nickel Thiolate Catalyst for the Long-Lived Photocatalytic Production of Hydrogen in a Noble-Metal-Free System. *Angewandte Chemie International Edition* **2012**, *51*, 1667-1670.

(34) Panagiotakis, S.; Landrou, G.; Nikolaou, V.; Putri, A.; Hardre, R.; Massin, J.; Charalambidis, G.; Coutsolelos, A. G.; Orio, M. Efficient Light-Driven Hydrogen Evolution Using a Thiosemicarbazone-Nickel (II) Complex. *Frontiers in Chemistry* **2019**, *7*.

(35) Lazarides, T.; McCormick, T.; Du, P. W.; Luo, G. G.; Lindley, B.; Eisenberg, R. Making Hydrogen from Water Using a Homogeneous System Without Noble Metals. *Journal of the American Chemical Society* **2009**, *131*, 9192-+.

(36) Kalyanasundaram, K.; Neumannspallart, M. Photophysical and Redox Properties of Water-Soluble Porphyrins in Aqueous-Media. *Journal of Physical Chemistry* **1982**, *86*, 5163-5169.

(37) Xu, Y.; He, C. C.; Liu, F. P.; Jiao, M. Z.; Yang, S. F. Hybrid hexagonal nanorods of metal nitride clusterfullerene and porphyrin using a supramolecular approach. *Journal of Materials Chemistry* **2011**, *21*, 13538-13545.

(38) Rochford, J.; Chu, D.; Hagfeldt, A.; Galoppini, E. Tetrachelate porphyrin chromophores for metal oxide semiconductor sensitization: Effect of the spacer length and anchoring group position. *Journal of the American Chemical Society* **2007**, *129*, 4655-4665.

(39) Venkatramaiah, N.; Pereira, C. F.; Mendes, R. F.; Paz, F. A. A.; Tome, J. P. C. Phosphonate Appended Porphyrins as Versatile Chemosensors for Selective Detection of Trinitrotoluene. *Analytical Chemistry* **2015**, *87*, 4515-4522.

(40) Shetti, V. S.; Ravikanth, M. A simple alternative method for preparing Sn(IV) porphyrins. *Journal of Porphyrins and Phthalocyanines* **2010**, *14*, 361-370.

(41) Thomas, A.; Kuttassery, F.; Mathew, S.; Remello, S. N.; Ohsaki, Y.; Yamamoto, D.; Nabetani, Y.; Tachibana, H.; Inoue, H. Protolytic behavior of axially coordinated hydroxy groups of Tin(IV) porphyrins as promising molecular catalysts for water oxidation. *Journal of Photochemistry and Photobiology a-Chemistry* **2018**, *358*, 402-410.

(42) Manke, A. M.; Geisel, K.; Fetzer, A.; Kurz, P. A water-soluble tin(IV) porphyrin as a bioinspired photosensitiser for light-driven proton-reduction. *Physical Chemistry Chemical Physics* **2014**, *16*, 12029-12042.

(43) Soman, R.; Raghav, D.; Sujatha, S.; Rathinasamy, K.; Arunkumar, C. Axial ligand modified high valent tin(IV) porphyrins: synthesis, structure, photophysical studies and photodynamic antimicrobial activities on Candida albicans. *Rsc Advances* **2015**, *5*, 61103-61117.

(44) Sobczynski, J.; Tonnesen, H. H.; Kristensen, S. Influence of aqueous media properties on aggregation and solubility of four structurally related meso-porphyrin photosensitizers evaluated by spectrophotometric measurements. *Pharmazie* **2013**, *68*, 100-109.

(45) Pavlishchuk, V. V.; Addison, A. W. Conversion constants for redox potentials measured versus different reference electrodes in acetonitrile solutions at 25 degrees C. *Inorganica Chimica Acta* **2000**, *298*, 97-102.

(46) Harriman, A.; Richoux, M. C.; Neta, P. Redox Chemistry of Metalloporphyrins in Aqueous-Solution. *Journal of Physical Chemistry* **1983**, *87*, 4957-4965.

(47) Gabrielsson, A.; Smith, J. R. L.; Perutz, R. N. Remote site photosubstitution in metalloporphyrin-rhenium tricarbonylbipyridine assemblies: photo-reactions of molecules with very short lived excited states. *Dalton Transactions* **2008**, 4259-4269.

(48) Li, X. Q.; Wang, M.; Zhang, S. P.; Pan, J. X.; Na, Y.; Liu, J. H.; Akermark, B.; Sun, L. C. Noncovalent assembly of a metalloporphyrin and an iron hydrogenase active-site model: Photo-induced electron transfer and hydrogen generation. *Journal of Physical Chemistry B* **2008**, *112*, 8198-8202.

(49) Kim, J. H.; Lee, S. H.; Lee, J. S.; Lee, M.; Park, C. B. Zn-containing porphyrin as a biomimetic light-harvesting molecule for biocatalyzed artificial photosynthesis. *Chemical Communications* **2011**, *47*, 10227-10229.

(50) Razavet, M.; Artero, V.; Fontecave, M. Proton electroreduction catalyzed by cobaloximes: Functional models for hydrogenases. *Inorganic Chemistry* **2005**, *44*, 4786-4795.

(51) Du, P. W.; Schneider, J.; Luo, G. G.; Brennessel, W. W.; Eisenberg, R. Visible Light-Driven Hydrogen Production from Aqueous Protons Catalyzed by Molecular Cobaloxime Catalysts. *Inorganic Chemistry* **2009**, *48*, 4952-4962.

(52) Zoski, C. G.: Preface. In *Handbook of Electrochemistry*; Zoski, C. G., Ed.; Elsevier: Amsterdam, 2007; pp v-vi.

(53) Amemiya, S.; Arning, M. D.; Baur, J. E.; Bergren, A. J.; Chen, S.; Ciobanu, M.; Cliffel, D. E.; Creager, S.; Démaillé, C.; Denuault, G.; Dryfe, R. A. W.; Edwards, G. A.; Ewing, A. G.; Fan, F.-R. E.; Fernandez, J.; Forster, R. J.; Haram, S. K.; Holt, K. B.; Keyes, T. E.; Kucernak, A.; Lee, Y.; Liu, B.; Mauzeroll, J.; Miao, W.; Minteer, S. D.; Mirkin, M. V.; Penner, R. M.; Porter, M. D.; Shao, Y.; Smith, T. J.; Stevenson, K. J.; Swain, G. M.; Szunerits, S.; Ugo, P.; Tel-Vered, R.; White, H. S.; Wittenberg, N. J.; Zoski, C. G.: Corresponding Authors. In *Handbook of Electrochemistry*; Zoski, C. G., Ed.; Elsevier: Amsterdam, 2007; pp xix-xx.

(54) Rodenberg, A.; Orazietti, M.; Probst, B.; Bachmann, C.; Alberto, R.; Baldridge, K. K.; Hamm, P. Mechanism of Photocatalytic Hydrogen Generation by a Polypyridyl-Based Cobalt Catalyst in Aqueous Solution. *Inorganic Chemistry* **2015**, *54*, 646-657.

(55) Tian, H. N.; Oscarsson, J.; Gabrielsson, E.; Eriksson, S. K.; Lindblad, R.; Xu, B.; Hao, Y.; Boschloo, G.; Johansson, E. M. J.; Gardner, J. M.; Hagfeldt, A.; Rensmo, H.; Sun, L. C. Enhancement of p-Type Dye-Sensitized Solar Cell Performance by Supramolecular Assembly of Electron Donor and Acceptor. *Scientific Reports* **2014**, *4*.

(56) Wayner, D. D. M.; Dannenberg, J. J.; Griller, D. Oxidation Potentials of Alpha-Aminoalkyl Radicals - Bond-Dissociation Energies for Related Radical Cations. *Chemical Physics Letters* **1986**, *131*, 189-191.

(57) Stoe & Cie, X.-A., version 1.30: Program for the acquisition and analysis data, Stoe & Cie GmbH, Darmatadt, Germany, 2005.

(58) Stoe & Cie, X.-R., version 1.28b: Program for data reduction and absorption correction, Stoe &Cie GmbH, Darmatadt, Germany, 2005.

(59) Stoe & Cie, X.-S., version 2.05: Program for crystal optimization for numerical absorption correction, Stoe & Cie GmbH, Darmatadt, Germany, 2004.

(60) G. M. Sheldrick, A. C. A., 64, 112-122.

(61) S. G. M. Sheldrick, P. f. C. S. S., University of Göttingen, 2014.

(62) G. M. Sheldrick, S., Version 2014/7, Program for Crystal Structure Refinement, University of Göttingen, 2014.

(63) Macrae, C. F.; Edgington, P. R.; McCabe, P.; Pidcock, E.; Shields, G. P.; Taylor, R.; Towler, M.; van De Streek, J. Mercury: visualization and analysis of crystal structures. *Journal of Applied Crystallography* **2006**, *39*, 453-457.

(64) Deniaud, D.; Schollhorn, B.; Mansuy, D.; Rouxel, J.; Battioni, P.; Bujoli, B. Synthesis and Catalytic Properties of Manganese Porphyrins Incorporated into Phosphonate Networks. *Chemistry of Materials* **1995**, *7*, 995-1000.

(65) Odobel, F.; Blart, E.; Lagree, M.; Villieras, M.; Boujtita, H.; El Murr, N.; Caramori, S.; Bignozzi, C. A. Porphyrin dyes for TiO2 sensitization. *Journal of Materials Chemistry* **2003**, *13*, 502-510.

For Table of Contents Only

Herein, we present a series of zinc and tin porphyrins used as photosensitizers in photochemical hydrogen evolution utilizing cobaloxime complexes as molecular catalysts. We studied the impact of the charge of *para*-substituents of meso-phenyl groups of the porphyrin on the hydrogen production. Among all porphyrins tested, one positively charged zinc-porphyrin and three neutral tin-porphyrins were photocatalytically active. We examined all parameters that impact hydrogen evolution and determined the mechanism of photocatalysis.